JACS
JOURNAL OF THE AMERICAN CHEMICAL SOCIETY

Communication

pubs.acs.org/JACS

Probing Conformational Exchange Dynamics in a Short-Lived Protein Folding Intermediate by Real-Time Relaxation–Dispersion NMR

Rémi Franco,[†,‡,§] Sergio Gil-Caballero,[∥] Isabel Ayala,[†,‡,§] Adrien Favier,[†,‡,§] and Bernhard Brutscher*[,†,‡,§]

[†]Institut de Biologie Structurale, Université Grenoble Alpes, 71 Avenue des Martyrs, 38044 Grenoble Cedex 9, France
[‡]Commissariat à l'Energie Atomique et aux Energies Alternatives (CEA), Grenoble, France
[§]Centre National de Recherche Scientifique (CNRS), Grenoble, France
[∥]Instituto de Investigaciones Químicas (CSIC/US), Sevilla, Spain

Supporting Information

ABSTRACT: NMR spectroscopy is a powerful tool for studying molecular dynamics at atomic resolution simultaneously for a large number of nuclear sites. In this communication, we combine two powerful NMR techniques, relaxation–dispersion NMR and real-time NMR, in order to obtain unprecedented information on the conformational exchange dynamics present in short-lived excited protein states, such as those transiently accumulated during protein folding. We demonstrate the feasibility of the approach for the amyloidogenic protein β2-microglobulin that folds via an intermediate state which is believed to be responsible for the onset of the aggregation process leading to amyloid formation.

Atomic resolution information on the structure and dynamics of biological macromolecules and their complexes is mandatory in order to understand biological function at the molecular level. Over the past decades, structural biologists have produced an impressive amount of high-resolution structural information on ground-state conformations of proteins and other biomolecules. It has long been recognized, however, that biomolecules are dynamic ensembles rather than static entities and that alternative high-energy conformations can play important functional roles,[1−4] or may be responsible for the onset of misfolding and aggregation leading to cellular deregulation and disease.[5−7] Therefore, there is a need for experimental techniques that provide access to the folding free-energy landscape of biomolecules in terms of conformational dynamics and structural properties corresponding to local energy minima. The short lifetime and/or low population of such excited states make them invisible for conventional high-resolution structural techniques. NMR spectroscopy is unique in its ability to study conformational dynamics over a wide range of time scales, from picoseconds to hours, simultaneously for a large number of individual nuclear sites in the molecule. In particular, low-populated excited states that are separated from the ground state by kinetic barriers leading to interconversion on the micro- to millisecond time scale can be accessed by relaxation–dispersion (RD) NMR, while states involving even higher energy barriers are best studied by real-time NMR methods. In this communication, we present a combination of these two powerful NMR techniques, real-time RD NMR that enabled the detection of conformational exchange dynamics in the major folding intermediate of the amyloidogenic protein β2-microglobulin (B2M) with a half-life time of about 20 min.

Although the basics have been developed since the 1950s, RD NMR has only recently evolved into a versatile technique to study the conformation of exited protein states.[9,10] A relaxation-compensated Carr–Purcell–Meiboom–Gill (CPMG)-based RD NMR experiment for backbone ^{15}N nuclei in proteins[11] is shown in Figure 1a. In this experiment, the dependence of ^{15}N transverse relaxation rates on the rate by which chemical shift evolution is refocused is measured by recording a series of 2D ^{1}H–^{15}N correlation spectra with a

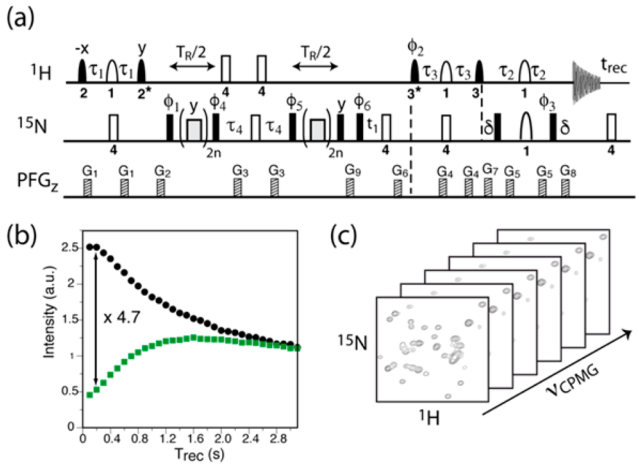

Figure 1. (a) NMR pulse sequence of the BEST-TROSY CPMG relaxation-dispersion (RD) experiment. More details are provided in the Supporting Information. (b) Experimental evaluation of the sensitivity of the BEST-TROSY experiment (black dots) compared to a standard TROSY-based[8] CPMG-RD version (green dots). Data were recorded on a ubiquitin sample (15 °C, 600 MHz, T_R = 60 ms). (c) For BEST-TROSY CPMG RD, a series of 2D ^{1}H–^{15}N spectra are recorded for different CPMG frequencies (180° pulse spacing) in a 3D-type experiment.

Received: November 23, 2016
Published: January 9, 2017

DOI: 10.1021/jacs.6b12089
J. Am. Chem. Soc. 2017, 139, 1065−1068

varying number of 180° ^{15}N pulses applied during a fixed relaxation delay T_R. The RD profiles obtained for individual ^{15}N nuclei can then be fitted to obtain information on the lifetimes of the exchanging states, their relative populations, and the chemical shift differences between them. In order to make this CPMG-RD experiment compatible with real-time NMR, where a full data set needs to be recorded during the lifetime of a transiently populated state, we have implemented the BEST-TROSY[12] approach in the CPMG-RD experiment. BEST-TROSY (BT) is a fast-pulsing technique, we have recently introduced to increase the speed and sensitivity of ^{1}H detected 2D and 3D heteronuclear correlation experiments of proteins[13] and nucleic acids.[14] The resulting BT-CPMG-RD experiment results in a significantly enhanced experimental sensitivity for short interscan delays (t_{rec}), resulting in reduced overall acquisition times as required for real-time NMR applications. Bench-marking the experiment on a sample of ubiquitin yields an average sensitivity increase of more than a factor of 4 using an optimized interscan delay of 200 to 300 ms (Figure 1b). Note that the actual sensitivity improvement will depend on the molecular size (rotational correlation time), the magnetic field strength, as well as the chosen relaxation delay.[12] Accurate measurements require the NMR instrumentation to be stable over the experimental duration. In the context of BT-CPMG-RD, this is a nontrivial issue, as the radio frequency load in the NMR probe varies significantly as a function of the CPMG pulse rate, and the use of short interscan delays reduces the duty cycle. We therefore have first tested the performance of the experiment on NMR spectrometers equipped with last-generation cryogenic probes. The results obtained for ubiquitin (Figure S2) show that flat RD profiles are obtained, as expected for ubiquitin, even at high repetition rates (short interscan delays). Consequently, the new BT-CPMG-RD experiment combined with modern cryogenic probe technology enables the application of RD NMR to low-quantity or timely unstable protein samples and reduces the overall time requirements for conventional applications, typically requiring data recording at multiple magnetic field strengths. Most interestingly, however, BT-CPMG-RD can be used to characterize the conformational dynamics present in transiently populated conformational protein states, as we will demonstrate in the following.

β2-Microglobulin (B2M), the light chain of the human class I major histocompatibility complex, forms amyloid fibrils in the joints and connective tissues of patients undergoing long-term dialysis (amyloidosis). B2M has been studied for some time as a model system in order to better understand the relationship between protein folding and amyloid formation.[15−19] In particular, a long-lived folding intermediate (I-state) has been identified that is believed to be involved in the onset of the disease.[18] Recently, we could show by a variety of NMR and other biophysical methods that the I-state of B2M has a higher affinity for dimerization than the N-state.[20] We have also shown that the I-state of B2M is amenable to real-time 2D and 3D NMR investigation.[21] In our initial real-time NMR study of the B2M mutant W60G,[22] which was preferred over the wild-type protein because of a higher I-state population after the refolding burst phase, we obtained partial NMR backbone resonance assignments, and we could detect increased ^{15}N transverse relaxation rates in parts of the protein which globally retains a native-like fold.[21] In order to determine whether the increase in transverse relaxation is caused by conformational exchange dynamics in this short-lived I-state ($t_{1/2}$ = 20 min) we now performed real-time BT-CPMG-RD measurements with the pulse sequence of Figure 1a. The experiment creates a three-dimensional (3D) data set with two chemical shift (^{1}H, ^{15}N), and one CPMG frequency dimensions (Figure 1c). Therefore, the same experimental strategy as previously described for 3D assignment experiments[21,23] has been applied (Figure S3). In short, two data sets are recorded, the first one during the refolding process (real-time spectrum), and a second one after the folding is completed (steady-state spectrum). A pure I-state spectrum is then obtained as the difference between the real-time data and the steady-state data that has been apodized to account for the refolding kinetics, and the different acquisition times. In our study, the folding rate constant k_f was known from previous SOFAST-based[19,21] experiments. If this information is unknown it can also be obtained from an initial guess, followed by an iterative optimization procedure.[21]

For real-time NMR, the protein folding reaction is initiated by fast mixing of a B2M-W60G solution at low pH, where the protein is in an unfolded state, with a refolding buffer in which the protein adopts after some time its native state. This mixing of solutions inside the NMR magnet (in situ) is experimentally achieved by an appropriate injection device (Figure S3).[24,25] Intramolecular disulfide bond formation was experimentally verified for each B2M sample. 3D BT-CPMG-RD spectra of the I-state of B2M-W60G (sample concentration of 0.5−0.6 mM) were recorded at magnetic field strengths of 16.5 T (700 MHz) and 20 T (850 MHz) in an overall experimental time of 50 min for the real-time data and 20 to 40 h for the steady state data. The relaxation delay was fixed to T_R = 20 ms, and 7 CPMG frequency points from 100 to 1000 Hz were sampled together with a reference point where the relaxation delay is omitted. More details on the experimental setup are given in the Supporting Information. The reference plane of the reconstructed I-state spectrum at 700 MHz, shown in Figure 2, illustrates the quality of the obtained data. In contrast to the N-state of B2M-W60G that shows a quite uniform peak intensity

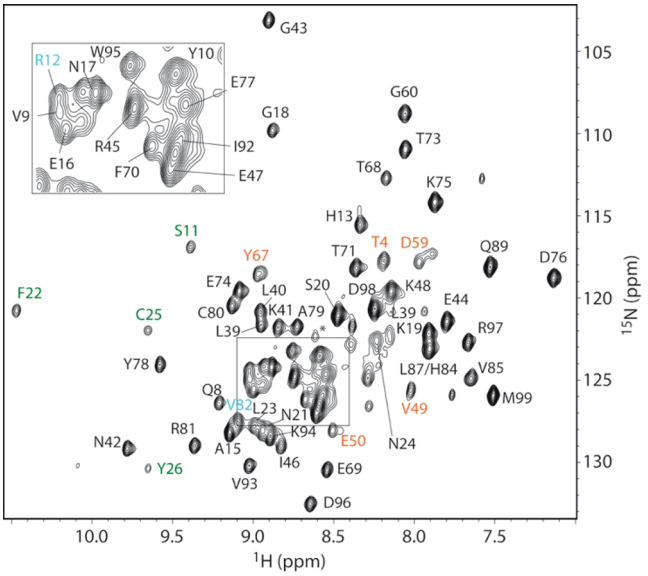

Figure 2. Reconstructed pure I-state BT-CPMG-RD spectrum of B2M-W60G recorded at 15 °C, 700 MHz. Shown is the reference plane (no relaxation delay) extracted from the 3D data set. The assigned cross peaks are annotated by the corresponding residue type and number. Residues for which conformational exchange is detected are color-coded.

DOI: 10.1021/jacs.6b12089
J. Am. Chem. Soc. 2017, 139, 1065−1068

distribution (Figure S4), no cross peaks are detected for a number of residues in the I-state, clustering in a protein region close to P32 (Figure 3a) that adopts a non-native *trans* peptide

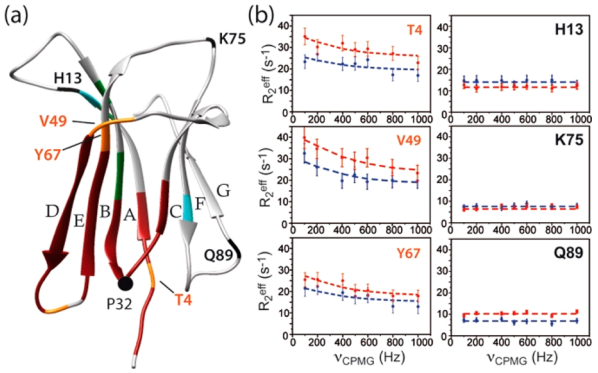

Figure 3. (a) Cartoon structure of B2M-W60G (PDB entry 2Z9T).[22] The β-strand arrangement is annotated by capital letters (A–G). I-state residues not detected in the NMR spectra due to extreme line broadening, are color-coded in red, while residues with strong line broadening, and nonflat RD profiles are highlighted in green (large R_{ex}), orange (medium R_{ex}), and cyan (small R_{ex}). All residues with flat RD curves are shown in gray. Amide sites for which CPMG-RD data are shown in (b) are annotated by the corresponding residue number and amino-acid type. (b) CPMG-RD data measured at 700 MHz (blue) and 850 MHz (red) for selected residues of the I-state of B2M-W60G.

bond in the I-state. The absence of NMR signal indicates the presence of conformational exchange processes in this folding intermediate. Interestingly, a couple of residues in this part of the protein still give rise to detectable NMR signals, although they show significant line broadening. RD NMR thus provides an experimental tool to prove the presence of such millisecond time scale motion and, eventually, further characterize them in terms of exchange kinetics and thermodynamics.

For the I-state of B2M-W60G, flat dispersions are observed in the 3D BT-CPMG-RD spectra for residues located on the protein side opposite of P32, as well as for most residues in β-strands F and G, while a total of 11 amide sites, all located close to the protein region where NMR signals are broadened beyond detection, show significant line broadening and relaxation dispersion. Examples of CPMG-RD profiles extracted for a selection of residues in the I-state are plotted in Figure 3b. The observed line-broadening effects can be classified into different categories, as indicated by color coding in Figures 2 and 3a: residues without observable line broadening (gray), residues showing very small, but measurable relaxation-dispersion (cyan), residues with significant relaxation dispersion (orange), residues with detectable $^1H-^{15}N$ correlation peaks but very low SNR (green), and finally residues for which no amide correlation peak could be detected in any NMR experiment (dark red).

The observed CPMG dispersions may be caused either by intramolecular conformational dynamics or by a monomer–dimer exchange process due to transient protein interactions mainly localized at the BC and DE loops at the apical site (close to P32) of B2M as previously observed for the wild-type protein,[20] the ΔN6 mutant,[17] as well as combinations thereof.[26] In order to discriminate between the two models, we have performed additional real-time experiments to investigate the dependence of NMR chemical shifts and line widths on the protein concentration (Figure S5). At 750 MHz ^1H frequency, we observe concentration-dependent peak shifts very similar to what has been previously reported for the B2M ΔN6 mutant[17] that is considered a valuable equilibrium analogue of the I-state. Furthermore, differential line broadening is significantly increased at 850 MHz, indicative of a monomer–dimer exchange rate of a few thousand per second. Unfortunately, in this fast exchange regime, a global fit of our relaxation–dispersion data to a two-state exchange model leads to unreliable results, as the fit parameters (chemical shift differences, exchange rate, and dimer population) are highly correlated. Therefore, we had to make some additional assumptions: (i) small chemical shift changes (<1 ppm) as most observed residues are far away from the dimer interface, and (ii) a dimer population of 20%. This estimation is based on a combination of previous findings: a dimer population of 50% for the I-state of wild-type B2M,[20] and the comparison of real-time NMR data recorded for wild-type and W60G B2M indicating a 2.5-fold lower I-state dimer population for the latter.[19] With these assumptions, a global fit of the CPMG-RD profiles yields an exchange rate k_{ex} = 2400 ± 500 s^{-1}, in good qualitative agreement with the data presented in Figure S5, and chemical shift changes of 0.7–1.0 ppm (T4, V49, E50, D59, Y67), 0.5 ppm (V82), and 0.3 ppm (R12). Interestingly, the monomer–dimer exchange kinetics in the I-state are at least 1 order of magnitude faster than in the N-state (Figure S6). This allows us to draw some conclusions on the energy barriers between monomeric and dimeric B2M-W60G in the I-state as compared to the N-state (Figure 4). The faster exchange

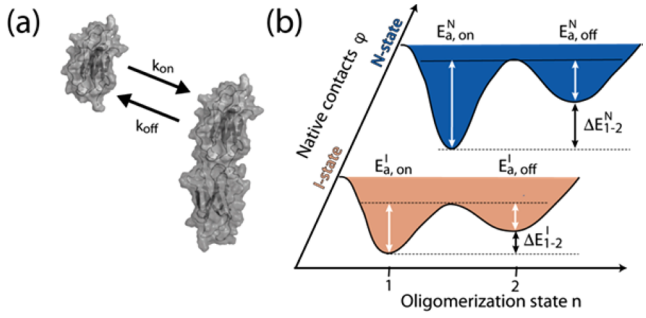

Figure 4. (a) B2M monomer–dimer equilibrium. B2M dimers have been shown to involve a head-to-head interaction with the side of P32 at the dimer interface[20] (b) Sketch of the free energy landscape of B2M-W60G plotted as a function of 2 variables: the degree of native-state structure φ, and the oligomerization state (n = 1: monomer, n = 2: dimer). Only the traces corresponding to the I-state and N-state minima are shown.

kinetics may be explained by a decrease in the transition state energy due to more favorable intermolecular contacts, a consequence of the presence of exposed hydrophobic side chains,[17,20] while the increased dimer population is mainly due to an increase in the free energy of the I-state monomer. These conclusions probably also hold true for wild-type B2M, although the absolute values for the energy barriers will be different, as well as the transition probability between the I- and N-states.[19,27] Our results are also in line with recent findings by Radford and co-workers,[26] who demonstrated that the formation of kinetically unstable B2M dimers favors amyloid assembly.

In summary, we have presented a sensitivity-optimized experiment for CPMG-based relaxation-dispersion NMR

DOI: 10.1021/jacs.6b12089
J. Am. Chem. Soc. 2017, 139, 1065–1068

measurements. This experiment, combined with state-of-the-art NMR hardware (high-field NMR magnets, last-generation cryogenic probes), and in situ real-time NMR techniques, provides a powerful new tool for site-resolved investigation of conformational dynamics occurring in timely unstable or transiently populated protein states. This has been demonstrated for a protein folding intermediate (I-state) of B2M-W60G. The BT-CPMG-RD experiment, presented here, will be equally useful for exploring the dynamics of other chemical moieties, such as aromatic $^{13}C-^{1}H$ spin pairs,[28,29] thus enlarging the application range of CPMG-RD real-time NMR to protein side chains and nucleic acid bases. We believe that the combination of multidimensional real-time and relaxation-dispersion NMR is a still challenging, but promising new experimental tool for characterizing the dynamics in excited states of macromolecules at atomic resolution.

■ ASSOCIATED CONTENT

Supporting Information

The Supporting Information is available free of charge on the ACS Publications website at DOI: 10.1021/jacs.6b12089.

Additional figures containing NMR spectra, and experimental procedures (PDF)

■ AUTHOR INFORMATION

Corresponding Author

*bernhard.brutscher@ibs.fr

ORCID

Bernhard Brutscher: 0000-0001-7652-7384

Notes

The authors declare no competing financial interest.

■ ACKNOWLEDGMENTS

We thank Dr. Paul Schanda for stimulating discussions. This work used the NMR platform of the Grenoble Instruct Centre (ISBG: UMS 3518 CNRS-CEA-UJF-EMBL) with support from FRISBI (ANR-10-INSB-05-02) and GRAL (ANR-10-LABX-49-01) within the Grenoble Partnership for Structural Biology (PSB).

■ REFERENCES

(1) Korzhnev, D. M.; Salvatella, X.; Vendruscolo, M.; Di Nardo, A. A.; Davidson, A. R.; Dobson, C. M.; Kay, L. E. *Nature* **2004**, *430*, 586−590.

(2) Boehr, D. D.; McElheny, D.; Dyson, H. J.; Wright, P. E. *Science* **2006**, *313*, 1638−1642.

(3) Henzler-Wildman, K.; Kern, D. *Nature* **2007**, *450*, 964−972.

(4) Kalodimos, C. G. *Protein Sci.* **2011**, *20*, 773−782.

(5) Dobson, C. M. *Semin. Cell Dev. Biol.* **2004**, *15*, 3−16.

(6) Chiti, F.; Dobson, C. M. *Annu. Rev. Biochem.* **2006**, *75*, 333−366.

(7) Soto, C. *J. Neurol. Transl. Neurosci.* **2013**, *1*, 1010.

(8) Loria, J. P.; Rance, M.; Palmer, A. G., III *J. Biomol. NMR* **1999**, *15*, 151−155.

(9) Sekhar, A.; Kay, L. E. *Proc. Natl. Acad. Sci. U. S. A.* **2013**, *110*, 12867−12874.

(10) Neudecker, P.; Robustelli, P.; Cavalli, A.; Walsh, P.; Lundström, P.; Zarrine-Afsar, A.; Sharpe, S.; Vendruscolo, M.; Kay, L. E. *Science* **2012**, *336*, 362.

(11) Loria, J. P.; Rance, M.; Palmer, A. G. *J. Am. Chem. Soc.* **1999**, *121*, 2331−2332.

(12) Favier, A.; Brutscher, B. *J. Biomol. NMR* **2011**, *49*, 9−15.

(13) Solyom, Z.; Schwarten, M.; Geist, L.; Konrat, R.; Willbold, D.; Brutscher, B. *J. Biomol. NMR* **2013**, *55*, 311−321.

(14) Farjon, J.; Boisbouvier, J.; Schanda, P.; Pardi, A.; Simorre, J.-P.; Brutscher, B. *J. Am. Chem. Soc.* **2009**, *131*, 8571−8577.

(15) Chiti, F.; Mangione, P.; Andreola, A.; Giorgetti, S.; Stefani, M.; Dobson, C. M.; Bellotti, V.; Taddei, N. *J. Mol. Biol.* **2001**, *307*, 379−391.

(16) McParland, V. J.; Kad, N. M.; Kalverda, A. P.; Brown, A.; Kirwin-Jones, P.; Hunter, M. G.; Sunde, M.; Radford, S. E. *Biochemistry* **2000**, *39*, 8735−8746.

(17) Eichner, T.; Kalverda, A. P.; Thompson, G. S.; Homans, S. W.; Radford, S. E. *Mol. Cell* **2011**, *41*, 161−172.

(18) Jahn, T. R.; Parker, M. J.; Homans, S. W.; Radford, S. E. *Nat. Struct. Mol. Biol.* **2006**, *13*, 195−201.

(19) Corazza, A.; Rennella, E.; Schanda, P.; Mimmi, M. C.; Cutuil, T.; Raimondi, S.; Giorgetti, S.; Fogolari, F.; Viglino, P.; Frydman, L.; Gal, M.; Bellotti, V.; Brutscher, B.; Esposito, G. *J. Biol. Chem.* **2010**, *285*, 5827−5835.

(20) Rennella, E.; Cutuil, T.; Schanda, P.; Ayala, I.; Gabel, F.; Forge, V.; Corazza, a; Esposito, G.; Brutscher, B. *J. Mol. Biol.* **2013**, *425*, 2722−2736.

(21) Rennella, E.; Cutuil, T.; Schanda, P.; Ayala, I.; Forge, V.; Brutscher, B. *J. Am. Chem. Soc.* **2012**, *134*, 8066−8069.

(22) Esposito, G.; Ricagno, S.; Corazza, A.; Rennella, E.; Gümral, D.; Mimmi, M. C.; Betto, E.; Pucillo, C. E. M.; Fogolari, F.; Viglino, P.; Raimondi, S.; Giorgetti, S.; Bolognesi, B.; Merlini, G.; Stoppini, M.; Bolognesi, M.; Bellotti, V. *J. Mol. Biol.* **2008**, *378*, 887−897.

(23) Rennella, E.; Brutscher, B. *ChemPhysChem* **2013**, *14*, 3059−3070.

(24) Mok, K. H.; Nagashima, T.; Day, I. J.; Jones, J. A.; Jones, C. J. V; Dobson, C. M.; Hore, P. J. *J. Am. Chem. Soc.* **2003**, *125*, 12484−12492.

(25) Schanda, P.; Forge, V.; Brutscher, B. *Proc. Natl. Acad. Sci. U. S. A.* **2007**, *104*, 11257−11262.

(26) Karamanos, T. K.; Kalverda, A. P.; Thompson, G. S.; Radford, S. E. *Mol. Cell* **2014**, *55*, 214−226.

(27) Camilloni, C.; Sala, B. M.; Sormanni, P.; Porcari, R.; Corazza, A.; De Rosa, M.; Zanini, S.; Barbiroli, A.; Esposito, G.; Bolognesi, M.; Bellotti, V.; Vendruscolo, M.; Ricagno, S. *Sci. Rep.* **2016**, *6*, 25559.

(28) Weininger, U.; Respondek, M.; Akke, M. *J. Biomol. NMR* **2012**, *54*, 9−14.

(29) Boisbouvier, J.; Brutscher, B.; Simorre, J.; Marion, D. *J. Biomol. NMR* **1999**, *14*, 241−252.

DOI: 10.1021/jacs.6b12089
J. Am. Chem. Soc. 2017, 139, 1065−1068